

# A NOVEL NOISE REMOVAL ALGORITHM FOR VERTICAL ARTIFACTS IN DIGITAL ELEVATION MODELS

Lucas C. Villa Real<sup>1\*</sup>, Jose Edgardo L. Aban<sup>2</sup> and Saiful A Husain<sup>2</sup>

<sup>1</sup>IBM Research Brazil, São Paulo, Brazil

[lucasvr@br.ibm.com](mailto:lucasvr@br.ibm.com)

<sup>2</sup>Universiti Brunei Darussalam

[edgardo.aban@ubd.edu.bn](mailto:edgardo.aban@ubd.edu.bn), [saiful.husain@ubd.edu.bn](mailto:saiful.husain@ubd.edu.bn)

\* Corresponding author: [lucasvr@br.ibm.com](mailto:lucasvr@br.ibm.com)

## ABSTRACT

Remote sensing is a technique which demands a large amount of analysis on data which may have been captured from a variety of sources. Common sources range from aerial vehicles equipped with scanning devices to sensors attached to satellites in space missions. The data acquisition, however, is commonly subject to the interference of external factors, such as particles in the atmosphere and clouds, which may lead to noise in the data. This paper presents a technique to detect the presence of such artifacts, as observed in some digital elevation model data, and an algorithm to patch them. A case study on the second version of the ASTER GDEM shows that the proposed algorithm is effective in the detection and patching of vertical artifacts and that it can be applied to different data sets in the realm of digital elevation models.

**Keywords:** noise removal, digital elevation model, remote sensing, image processing

## INTRODUCTION

Aligned with the concept of a smarter planet, the interest of governments and corporations to predict natural disasters and their impacts on the society and businesses has substantially increased. Moreover, the dissemination of high resolution data to describe features of the Earth is allowing computer models to simulate the likelihood of such events with a great level of details. Still, the processes involved in the data acquisition through remote sensing are susceptible to conditions that could affect the quality of that data, thereby compromising the accuracy of various simulations.

One type of data derived from remote sensing is the terrain elevation, also called digital elevation model (DEM). Commonly presented in a gridded format that is convenient to process and use, they can have different spatial resolutions and accuracy, depending on the techniques employed to sample the surface. (e.g.: satellite data, specialized radars, on-land survey)

The Shuttle Radar Topography Mission (SRTM) is one common data source for DEMs. It was launched by NASA in 2000 and covers the globe from latitudes around 60 degrees north and 56 degrees south at a horizontal resolution of 3 arc-seconds (or 90 meters at the Equator). The SRTM data was obtained through radar interferometry, and many data voids and elevation issues originated from inherent backscatter in radar were identified by the scientific community and have been fixed throughout the years (Jarvis et al., 2000). As a consequence, the SRTM DEM is regarded as a stable elevation data set for scientific computation (Huang et al., 2011).

In 2011, NASA and Japan's Ministry of Economy, Trade and Industry (METI) have jointly released the second version of the ASTER GDEM elevation model. Covering the globe at latitudes up to 83 degrees and at a 1 arc-second resolution, the GDEM presents itself as a potential replacement for SRTM. The ASTER GDEM data is obtained by the analysis of two stereo images captured from a pair of sensors aboard the Terra satellite (Jet Propulsion Laboratories, 2001). Images from different passes of the satellite are stacked and averaged to produce the elevation data. However, since the satellite does not cover the globe with the same number of passes, some regions might present higher accuracy than others. Errors may arise from cloud cover and snow, resulting on bad pixels that may have a rate up to 12%, depending on the criteria adopted to determine what is a bad pixel (Urai, Tachikawa and Fujisada, 2012). Therefore, a number of applications may not benefit from the use of the ASTER

GDEM v2 data set. That is the case of hydrology models that must rely on a good representation of the topography to calculate surface runoff, for example.

Given the intrinsic problems of the various data acquisition techniques, the elevation data needs to be preprocessed for the removal of bad pixels before they are used for scientific computation. This paper presents a novel algorithm to detect the presence of vertical artifacts (mostly produced by noise and cloud cover) in digital elevation models and to patch them. A case study with a noisy topography data extracted from ASTER GDEM v2 is presented, followed by an analysis of the achieved results and future work.

## **PRIOR ART**

Different techniques to remove artifacts from DEMs have been proposed in the literature (Falorni et al., 2005). For data containing just a small fraction of bogus pixels that are not particularly correlated, smoothing algorithms such as Gaussian Filtering and Wavelet Filtering (Gagnon and Jouan, 1997) are common approaches that typically present good results. More complex scenes that include clouds or large, interconnected groups of noisy pixels need to be processed by specialized methods that take into account the nature of the problem.

Stevenson, Sun and Mitchell (2009) have proposed a denoising method for 3D objects which preserves features such as sharp edges and corners. While suited for 3D objects, it has been successfully adapted to topographic data in projected coordinate systems. The algorithm works by triangulating the DEM, and then altering the positions of the vertices of the triangles by recalculating the orientation of the triangular faces' normal vector. The level of denoising is adjusted by two parameters: a threshold that establishes the sharpness of the features to be preserved, and the number of iterations that will determine how much the data will be changed. The algorithm is effective in the removal of noise, but dense cloud formations are interpreted as part of the topography and smoothed rather than removed.

Feng et al. (2004) present a cloud removal method in remote sensing images using homomorphism filtering. Based on the observation that thin cloud has low frequency and land surface has more details and is found more frequently, the low frequency part of the image can be reduced by a filter in the frequency domain through a Fourier Transformation. The filtered image can then be obtained by changing the image back to the spatial domain. Because the translation of the image between different domains is computationally expensive, the authors put forward an improved homomorphism filtering. Based on general theory of statistics, the transformations and the filtering are approximated with regional average in the spatial domain. Through that approach, thin cloud is removed on the whole for a number of images, although some information is lost due to averaging. Homomorphism filtering does not work appropriately for the removal of dense clouds, however.

It's clear from the prior art that a substitution-based method is required to remove large groups of noisy pixels, be they related to clouds or not. Said methods rely on a ground truth data set (spatially aligned with the original data set) from where the bogus elevation pixels are substituted. The patching algorithm proposed in this paper follows this concept, with the differentiation that only pixels classified as artifacts are modified.

## **VERTICAL ARTIFACT DETECTION ALGORITHM**

The classification of pixels as artifacts is performed based on comparisons between the source and the ground truth data sets. The idea developed is that both data sets should have a similar elevation average and standard deviation, granted they have the same number of pixels and cover the same geographic extents. Groups of pixels which deviate from that norm are considered to be noise. That is a sound assumption for data sets close to each other in time, as well as for natural environments and for small to medium-sized cities or villages.

The core of the algorithm is as follows. With a  $N \times N$  grid-moving window defined as  $G$  where  $N$  is an odd number, the algorithm scans a DEM  $D$  and compares it against the ground truth data set  $R$ ,

also called the reference data set. On each scan, the elevation differences between the two sets are calculated to determine the existence of artifacts in  $D$ .

Let  $\alpha$  be a multiplier and  $\sigma$  the standard deviation of a given data set, the maximum accepted difference between the central point of the two  $N \times N$  grids  $G_D$  and  $G_R$  is defined as:

$$M = (\sigma_{G_R} + |\bar{D} - \bar{R}|) * \alpha \quad (1)$$

If the difference between the two central points is less than  $M$ , then it is assumed that the central point in  $G_D$  does not constitute noise. Otherwise, a patch is applied to the point located at the center of the grid  $G_D$  according to the algorithm described in the next subsection.

The grid size hence determines how many features of the scene are considered in the comparison. Naturally, the size of  $N$  is directly related to the spatial resolution of the DEM: the higher its resolution is, the greater  $N$  may be. For example, in a DEM with a 1-meter horizontal spatial resolution, a  $3 \times 3$  grid would not be sufficiently large to cover the width of a street. The  $\alpha$  multiplier controls how much the algorithm tolerates noise. Values greater than 1 will disregard small disturbances in the DEM whereas values between 0 and 1 will lead to an increased number of cells considered artifacts.

### PATCHING ALGORITHM

If a pixel  $D_{i,j}$  is classified as artifact by the detection algorithm, a patch function determines its new value based on the pixel  $R_{i,j}$  from the reference data set: the difference  $\phi$  between  $R_{i,j}$  and one of its neighbors  $R_{x,y}$  is calculated, and  $D_{i,j}$  is then substituted by the value of its neighbor  $D_{x,y}$  added by  $\phi$ , provided that  $D_{x,y}$  is not classified as an artifact too.

If all neighbor cells around  $D_{i,j}$  are bogus, then a different patching function is applied: the value of the reference pixel  $R_{i,j}$  is summed to the difference of the global average of the two data sets  $D$  and  $R$ . That difference is taken into account because the base elevation of the two data sets may differ depending on the acquisition instruments used to produce the DEMs.

The patching function can be thus defined as:

$$D_{i,j} = \begin{cases} R_{i,j} + |\bar{D} - \bar{R}|, & \text{if all neighbor cells of } D_{i,j} \text{ are classified as artifacts} \\ D_{x,y} + (R_{i,j} - R_{x,y}), & \text{otherwise} \end{cases} \quad (2)$$

### ALGORITHM EVALUATION AND DISCUSSION

A scene of the ASTER GDEM v2 was obtained from a region in Brunei Darussalam in which a large amount of noise was identified. Part of that scene is depicted in perspective on Figure 1-A. The noise appears as peaks that are not removed by the standard filtering techniques such as Gaussian Filtering or averaging. Using an upscaled SRTM as a the reference data set, the proposed algorithm was applied to the noisy scene with a grid-moving window size of  $N=7$  and with a multiplier  $\alpha$  of value 1.0. The resulting DEM is shown on Figure 1-B.

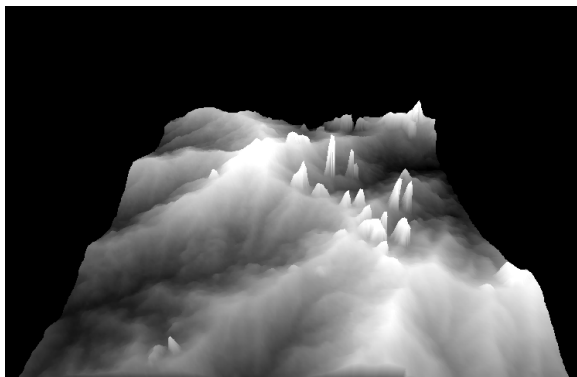


Figure 1-A: Noisy ASTER GDEM v2 data

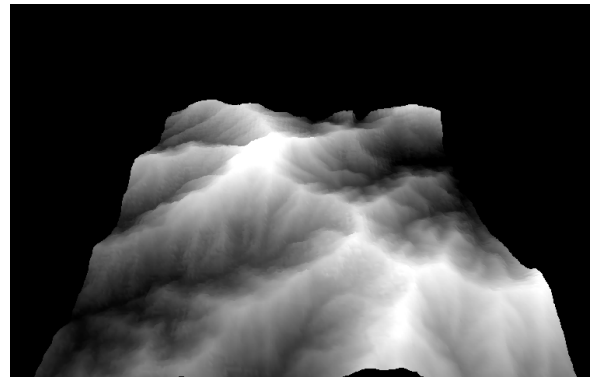


Figure 1-B: Patched ASTER GDEM

Through a visual inspection, it's possible to see that all the evident vertical artifacts pertaining to the ASTER GDEM were removed whilst preserving the overall features of the original data set. From the whole scene, 13% of the cells were considered to be noise by the artifact detection algorithm, which is a number very approximate to the maximum bad pixel rate identified by Urai, Tachikawa and Fujisada (2012) on the second version of the ASTER GDEM.

In order to compare the proposed algorithms with the classic approaches of data smoothing, a mean filter algorithm of sizes 3x3, 5x5 and 7x7 was applied to the same scene from ASTER GDEM v2. Mean filtering reduces the amount of intensity variation between one pixel and the next, effectively removing noise such as speckles. However, all cells of the DEM are potentially modified by this technique, which may be undesirable depending on the application.

One of the parameters used to assess the patching process was spectral profiling. Several image products were used in the process of witnessing the different data sets, namely the reference SRTM data set, the raw ASTER GDEM scene from Figure 1-A, the patched ASTER GDEM image, and the 3x3, 5x5, and 7x7 mean smoothed images.

In order to compare the performance of the different algorithms, image products were stacked as layers using the ERDAS Imagine software and selected pixels were assessed. The outcome was a pseudo composite image having 5 layers which include the three smoothed images described earlier. On each layer, the assessed pixels were analyzed by the *spectral profile viewer*, which allows for the visualization of their reflectance spectrum. This technique is particularly useful for hyperspectral data that can have hundreds of layers. Moreover, it allows estimates of the chemical composition of the material in the pixel. In more discrete applications, the technique can allow the user to compare the profiles that are generated to those from laboratory (or field) spectrophotometers. In this study, the technique was used to assess the behavior of patched and unpatched pixels in all the five image products mentioned above.

Ten (10) points of the areas that have been patched by the proposed algorithm were then compared among the different stacked layers. In Figure 2-A, the sample points picked from the pseudo-composite image are identified with a red placemark icon. The height values, derived from the 32-bit unsigned images and shown on Table 1, indicate that data smoothing is not appropriate for the removal of groups of vertical artifacts like the ones featured in the DEM processed. However, they remain useful as a post-processing filter to reduce the occurrence of small perturbances which are not identified by the detection algorithm presented in this paper.

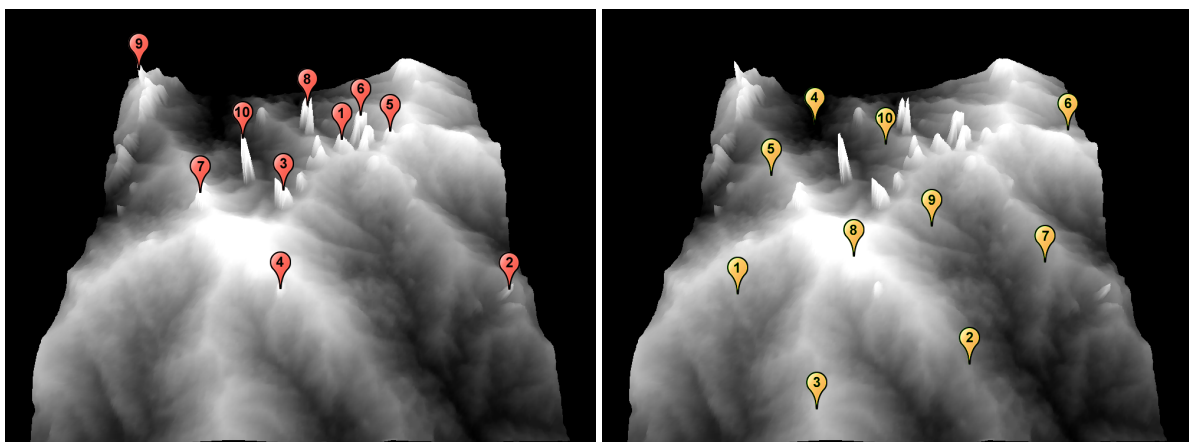


**Figure 2-A: Selected points picked from a set of SRTM-patched pixels for sampling.**

**Figure 2-B: Sample points selected from a set of pixels that were not patched.**

**Table 1. Sampled height values from patched points in different composite layers.**

Composite Layers	Sample 1	Sample 2	Sample 3	Sample 4	Sample 5	Sample 6	Sample 7	Sample 8	Sample 9	Sample 10
Raw ASTER	1954	1499	2298	1831	2028	2064	2118	2031	2246	2297
SRTM	1402	1011	1175	1623	1633	1146	1735	875	1434	768
Patched Grid	1410	1027	1169	1652	1641	1154	1753	883	1442	763
Mean Filtered Grid (3x3)	1942	1492	2170	1850	2035	2050	2080	1989	2237	2188
Mean Filtered Grid (5x5)	1925	1450	2019	1836	2020	2045	2050	1867	2171	1963
Mean Filtered Grid (7x7)	1893	1384	1841	1811	1992	2029	2009	1699	2086	1640

Likewise, 10 sampling points were also determined for areas that contained unpatched pixels. Figure 2-B shows the sample points randomly picked from the pseudo-composite image, identified by a yellow placemark icon. The values shown on Table 2 indicate the derived height values from the unpatched 32-bit unsigned images.

It's worth noting the elevation distance between the sampled pixels in the raw ASTER GDEM v2 and the SRTM reference data sets (which average 13.8 meters). When compared to the noisy values presented in Table 1 (whose distance averaged 656.4 meters), the heights assigned to the patched pixels in Table 1 indicate that the replacement algorithm can successfully maintain the shape of the reference data set and respect the base elevation of the two data sets at the same time: the average elevation distance between the sampled pixels of the patched and the SRTM grids is of 11.4 meters.

**Table 2. Sampled height values from unpatched points in different composite layers.**

Composite Layers	Sample1	Sample2	Sample3	Sample4	Sample5	Sample6	Sample7	Sample8	Sample9	Sample10
Raw ASTER	1727	692	1533	365	1183	1175	1262	2218	1469	881
SRTM	1736	726	1523	372	1198	1168	1261	2181	1481	887
Patched Grid	1727	692	1533	365	1183	1175	1262	2218	1469	881
Mean Filtered Grid (3x3)	1719	699	1533	361	1190	1190	1259	2222	1463	894
Mean Filtered Grid (5x5)	1717	704	1530	360	1180	1189	1260	2226	1455	902
Mean Filtered Grid (7x7)	1710	709	1523	357	1173	1188	1259	2228	1446	909

The sampling points and their corresponding pixel/height values in each of the representative layers are also plotted as series of spectral profiles on Figures 3 and 4.

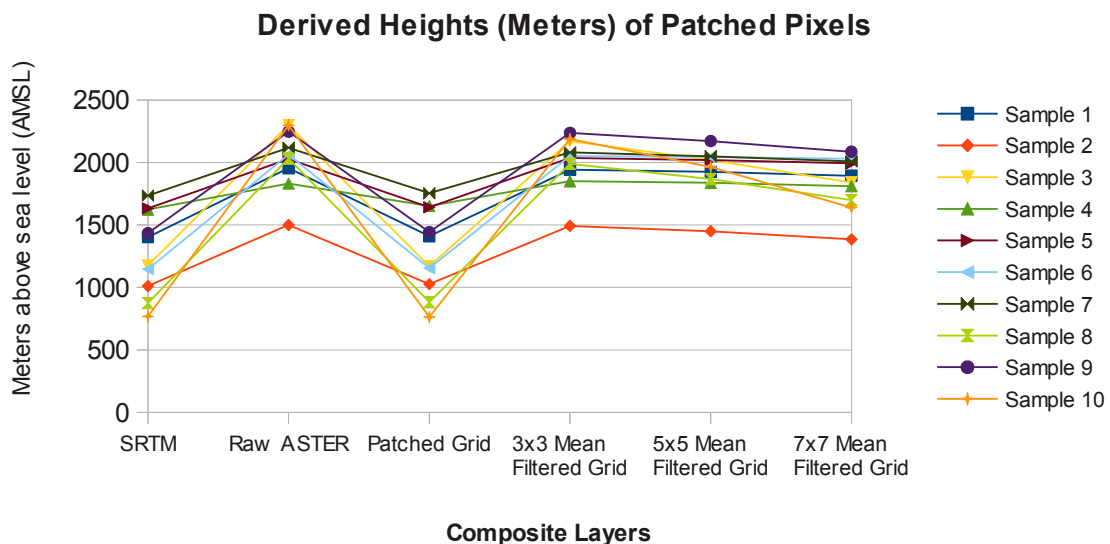


**Figure 3: Comparison of spectral profiles/height profiles for the pseudo-composite layer for selected SRTM-patched areas/pixels.**

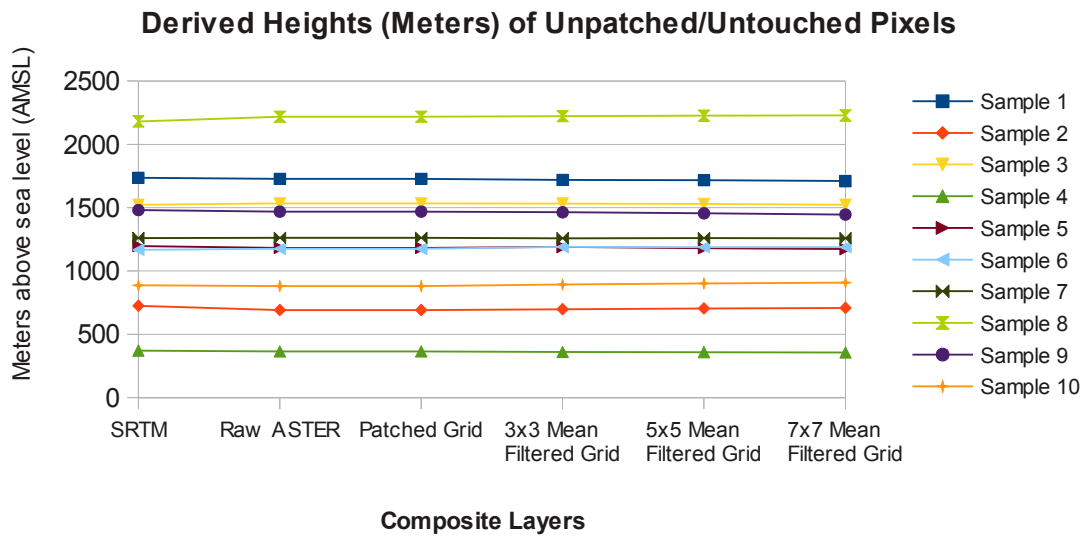


**Figure 4: Comparison of spectral profiles / height profiles for the pseudo-composite layer for selected unmodified pixels.**

## CONCLUSION

This paper presented a novel algorithm for the detection of vertical artifacts in digital elevation models and for the patching of pixels determined as such. An analysis of the performance of the algorithm was executed against the second version of the ASTER GDEM (with a horizontal resolution of 30 meters), having SRTM (sampled from 90 to 30-meter resolution) as reference data set. Post-processing validation and comparisons of the image products showed the effectiveness of the algorithm in removing the visibly noisy artifacts, while at the same time preserving the spatial and height characteristics of neighboring cells. The final DEM product derived from the patching process shows that the algorithm can efficiently salvage the high resolution properties of noisy data sets.

Possible improvements to specific file formats could also be made by implementing a content-aware version of the algorithm through the incorporation of meta-data from the DEM (provided that it exists). On a LiDAR-derived DEM, for instance, the elevation data can be accompanied by meta-data such as the intensity of the signal (the return strength of the laser pulse) and the return number from a single given pulse. In that case, the detection of artifacts could be heightened by e.g.: letting only points with a single return to be evaluated by the algorithm, or by preventing urban features such as tall buildings and towers from being detected as noise (Priestnall, Jaafar and Duncan, 2000).

Another content-aware version of the artifact detection technique could include the processing of ASTER meta-data: each elevation file obtained from the ASTER GDEM v2 has an associated QA (Quality Assurance) file that is also available for download. The QA file indicates how many ASTER scenes were used to estimate the elevation of a certain cell. Also, there are situations in which the ASTER GDEM may come with cells whose elevation were not estimated through stereo pairs (either because of noise, data voids, too little ASTER scenes available or other reasons). In such cases the QA data set will indicate which source was used to estimate their elevation (e.g.: SRTM or GTOPO30). Even though the location of the noisy artifacts evaluated in this paper did not coincide with regions poorly covered, the use of the QA data set could be positive for other regions around the globe.

Although improvements to deal with specific file formats and data sets are discussed in this section, a content-agnostic algorithm such as the presented one produces very satisfactory results without data requirements besides the elevation, thereby enabling the immediate use of unheeded digital elevation models on a large number of applications.

## REFERENCES

- Falorni, G., V. Teles, E. R. Vivoni, R. L. Bras, K. S. Amaratunga, 2005, Analysis and characterization of the vertical accuracy of digital elevation models from the Shuttle Radar Topography Mission, *Journal of Geophysical Research: Earth Surface* (110)
- Feng C., Ma J.-W., Dai Q., Chen X., 2004, An Improved Method for Cloud Removal in ASTER Data Change Detection, *International Geoscience and Remote Sensing Symposium* (5), 3387 – 3389
- Gagnon, L., Jouan, A., 1997, Speckle Filtering of SAR Images: a comparative study between complex-wavelet-based and standard filters. *SPIE Proceedings* (3169), 80 – 91
- Huang X., Xie H., Liang T., Yi D., 2011, Estimating vertical error of SRTM and map-based DEMs using ICESat altimetry data in the eastern Tibetan Plateau, *International Journal of Remote Sensing* 09/2011, 32(18), 5177 – 5196.
- Jarvis, A., H.I. Reuter, A. Nelson, E. Guevara, 2008, Hole-filled SRTM for the globe version 4, Available online: <http://srtm.csi.cgiar.org> (accessed on Sep 1<sup>st</sup>, 2013)
- Jet Propulsion Laboratories, 2001, ASTER Higher-Level Product User Guide, Available online: [http://asterweb.jpl.nasa.gov/content/03\\_data/04\\_Documents/ASTERHigherLevelUserGuideVer2May01.pdf](http://asterweb.jpl.nasa.gov/content/03_data/04_Documents/ASTERHigherLevelUserGuideVer2May01.pdf) (accessed on Sep 1<sup>st</sup>, 2013)
- Priestnall G., Jaafar J., Duncan A., 2000, Extracting urban features from LiDAR digital surface models, *Computers, Environment and Urban Systems*, (24)(2), 65 – 78
- Stevenson, J. A., Sun, X., Mitchell, N. C., 2010, Despeckling SRTM and other topographic data with a denoising algorithm, *Geomorphology* (114) (3), 238 – 252
- Urai M., Tachikawa, T., Fujisada, H., 2012, Data Acquisition Strategies for ASTER Global DEM Generation, *ISPRS Annals of the Photogrammetry and Remote Sensing and Spatial Information Sciences*, (I-4), 199 – 202.